Mol. Cryst. Liq. Cryst., Vol. 564: pp. 56–66, 2012

ISSN: 1542-1406 print/1563-5287 online
DOI: 10.1080/15421406.2012.691682

Taylor & Francis
Taylor & Francis Group

Numerical Analysis and Experiment on Discharge Characteristics Under Various Address Electrode Widths in AC Plasma Display Panel

CHOON-SANG PARK,[1] JAE YOUNG KIM,[2]
EUN YOUNG JUNG,[3] AND HEUNG-SIK TAE[1,*]

[1]School of Electronics Engineering, College of IT Engineering, Kyungpook National University, Daegu 702-701, Korea
[2]Holcombe Department of Electrical and Computer Engineering, Center for Optical Materials Science and Engineering Technologies (COMSET), Clemson University, Clemson, SC 29634, USA
[3]Core Technology Lab., Corporate R&D Center, Samsung SDI Company Ltd., Cheonan, Chungcheongnam-Do 330-300, Korea

The address-electrode width is an important parameter to affect both the address and sustain discharge characteristics in an ac-plasma display panels (ac-PDPs). It was numerically founded that as the address-electrode width was wider, the capacitance between the sustain and address electrodes (=C_{AY}) increased, but the capacitance between the two sustain electrodes (=C_{XY}) decreased. The resultant changes in the sustain and address discharge characteristics, such as a firing voltage, discharge delay time, and luminance, were examined in the 50 in ac-PDP with a high Xe (>11%) content. The increase in the address-electrode width caused an increase in the firing voltage between the sustain electrodes, which was mainly due to the decrease in the capacitance between two sustain electrodes and the increase in the wall charges accumulation toward the address electrode. In particular, the luminance was observed to increase with an increase in the address-electrode width. As the address-electrode width became broaden, the sustain discharge path was longer toward the address electrode, thereby enlarging the discharge volume. Therefore, it was observed that the IR (VUV) and Ne emissions were increased considerably. Furthermore, these experimental results were confirmed by simulating the electric field strength and Xe ion distribution in discharge cell with respect to the address-electrode width.

Keywords Address width; luminance; firing voltage; address delay time; spectral intensity; electric field; Xe ion; IR emission

1. Introduction

It is well-known that the wider address-electrode width could produce faster and more stable discharge [1]. This phenomenon can be explained in terms of the capacitance change in the rear panel induced by the variation in the width of address electrode. However, it is also found that the change in the address-electrode width can affect both the capacitances not

*Address correspondence to Prof. Heung-Sik Tae, School of Electronics Engineering, College of IT Engineering, Kyungpook National University, Sangyuk-dong, Buk-gu, Daegu 702–701, Korea (ROK). Tel: (+82)53-950-6563; Fax: (+82)53-950-5505. E-mail: hstae@ee.knu.ac.kr

only between the sustain and address electrodes but also between the two sustain electrodes [2], implying that the variation in the address-electrode width can affect both the address and sustain discharge characteristics of an AC-PDP. From a viewpoint of PDP driving, this would provide a possibility of the independent control over the sustain and plate-gap discharges.

Accordingly, in this paper, the cell capacitance variation was calculated as a function of the address-electrode width. The resultant changes in the sustain and address discharge characteristics, such as a firing voltage, discharge delay time, luminance, spectral intensity, electric field strength, and Xe ion distribution were examined in the 50 inch ac-PDP with a high Xe (>11%) content.

2. Simulation and Experimental Setup

2.1 Simulation Setup for Capacitance Calculation

Figure 1(a) shows a schematic diagram of single pixel from the 50 inch HD AC-PDP employed in this experiment. Figure 1(b) shows the capacitances between the X-Y electrodes, and between the A-Y electrodes in the single PDP cell, where X is the sustain electrode, Y is the scan electrode, and A is the address electrode. In order to calculate the cell capacitance, the Trefftz method in ANSYS simulation code was employed as a numerical method. The

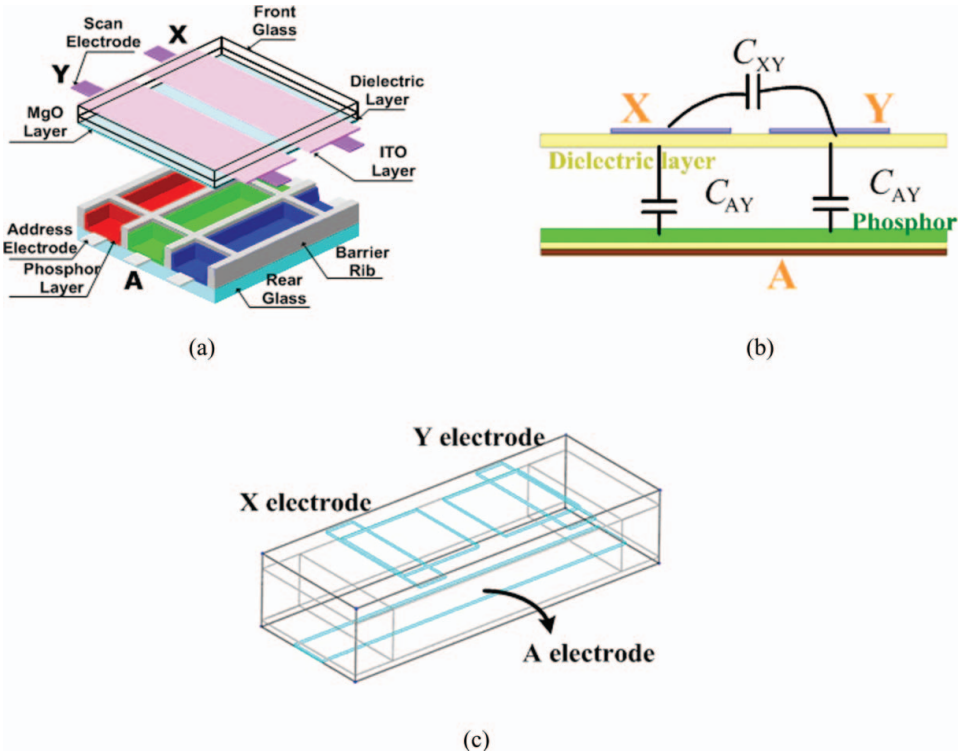

Figure 1. Schematic diagrams of (a) single pixel structure in 50 inch HD AC-PDP, (b) capacitances of between X-Y and A-Y electrodes in PDP cell, and (b) cell structure used in calculation of capacitance.

Table 1. Geometrical parameters for calculation of capacitance

	Parameter	Specification
Cell	Cell pitch	810 μm × 175 μm
Sustain electrode	Width/gap	200 μm/70 μm
Address electrode	Width	60, 90, 120,150 μm
Barrier rib	Height	120 μm
	Upper/lower width	25 μm/50 μm
	Permittivity	20
Front dielectric layer	Thickness	35 μm
	Permittivity	13
Rear dielectric layer	Thickness	15 μm
	Permittivity	20
Phosphor	Lateral thickness	30 μm
	Lower thickness	10 μm

cell capacitance is calculated by Eq. (1) [2].

$$
\begin{aligned}
C &= \frac{Q}{V}(C/V \, or \, F) \\
Q &= \int_S \rho_S ds = \int_S \varepsilon \hat{n} \cdot E ds = \int_S \varepsilon E \cdot ds \\
V &= V_{12} = -\int_{P_2}^{P_1} E \cdot dl \\
\therefore C &= \frac{Q}{V} = \frac{\int_S \varepsilon E \cdot ds}{-\int_l E \cdot dl}(F)
\end{aligned} \tag{1}
$$

The geometrical parameters for capacitance calculation are listed in detail in Table 1. The schematic diagrams of the cell structure and specifications used in our 3-D simulation are indicated in Fig. 1(c) and Table 2, respectively. The address-electrode width was varied

Table 2. Specifications for 3-D simulation used in this study

Parameter	Specification
Cell pitch	810 μm × 175 μm
Sustain electrode (width/gap)	200 μm/75 μm
Gas mixtures	Ne-Xe 15%, 500 Torr
Barrier rib height	120 μm
Front dielectric layer	
Thickness	35 μm
Permittivity	13
Rear dielectric layer	
Thickness	15 μm
Permittivity	15
Driving condition	Sustain 166 kHz

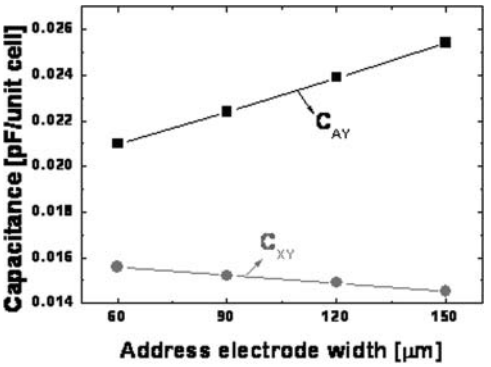

Figure 2. Comparison of capacitances between two sustain electrodes (C_{XY}) and between sustain and address electrodes (C_{AY}) per unit cell under various address electrode widths.

from 60 to 150 μm at the intervals of 30 μm. Figure 2 and Table 3 show the resultant capacitances between the two sustain electrodes ($=C_{XY}$) and between the sustain and address electrodes ($=C_{AY}$) per unit cell with respect to the address-electrode width. With an increase in the address-electrode width, the C_{XY} per unit cell decreased linearly from 0.0146 to 0.0135 [pF] ($\Delta C_{XY} = 0.0011$ pF), whereas the C_{AY} per unit cell increased from 0.0200 to 0.0244 [pF] ($\Delta C_{AY} = 0.0044$ pF). As shown in Fig. 2, the change in the address-electrode width induced the change of the capacitance, C_{AY}, affecting the address discharge, as well as the change of the capacitance, C_{XY}, affecting the sustain discharge. In this case, the change in the amount of the capacitance, C_{AY} was four times as large as that of the capacitance, C_{XY}, meaning that the variations in the address electrode width could affect the address discharge more considerably than the sustain discharge.

2.2 Experimental Setup for Measuring Discharge Characteristics

Figure 3 shows the optical-measurement systems and commercial 50 inch HD test panel with three electrodes used in this experiment. A color analyzer (CA-100 plus), driving circuit, waveform modification, photo-sensor amplifier (Hamamatsu, C6386), and spectrometer were used to measure the luminance, firing voltage, discharge delay time, IR emission, visible, and IR spectrum, respectively. A 50 inch panel with a working gas pressure of 450 Torr was employed in this study, and its structure and dimensions were an XGA grade PDP with a box-type barrier rib. The gas mixtures used were Ne-He (35%)-Xe (11%). Table 4 lists the detailed panel specifications for the test panel, which were exactly the same, except for the address-electrode width. Figure 4 shows the driving waveforms,

Table 3. Capacitances of C_{XY} and C_{AY} per unit cell under various address electrode widths

	Address electrode widths			
[pF]	60 μm	90 μm	120 μm	150 μm
X-Y	0.0146	0.0142	0.0141	0.0139
A-Y	0.0200	0.0214	0.0229	0.0244

Table 4. Specifications of 50 inch HD AC-PDP used in this study under various address electrode widths

Parameter	Specification
Cell pitch	808 μm × 175 μm
Rib height	120 μm
Gas mixtures	Ne-He 35%-Xe 11%
Pressure	450 Torr
ITO width	310 μm
ITO gap	60 μm
Address electrode width	60, 90, 120,150 μm

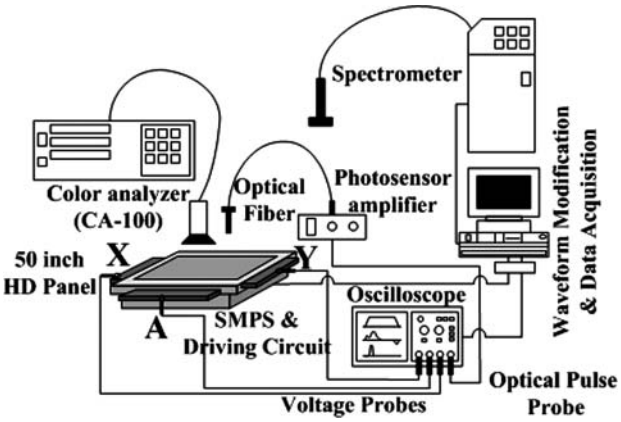

Figure 3. Schematic diagram of experimental setup employed in this paper.

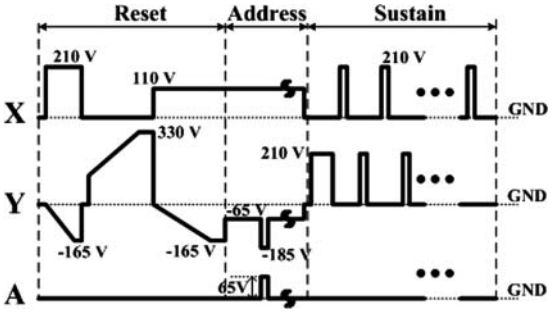

Figure 4. Schematic diagram of conventional driving waveform used in this paper.

including the reset, address, and sustain periods, employed to compare the discharge and luminance characteristics of the 50 inch test panels under various address electrode widths. The frequency for the sustain period was 200 kHz. A driving method with a selective reset waveform was also adopted.

3. Results and Discussion

3.1 Experimental Observation from 50 in Test Panel

To investigate the effects of cell capacitance caused by the address electrode width on both the address and sustain discharges, the experimental measurements were carried out under the 50 inch test panel with four blocks divided according to the address-electrode width ranging from 60 to 150 μm at the intervals of 30 μm.

Figure 5(a) shows the changes in the firing voltage between two sustain electrodes ($=V_{f(X\text{-}Y)}$) and the firing voltage between the sustain and address electrodes ($=V_{f(A\text{-}Y)}$) relative to the address-electrode width ranging from 60 to 150 μm. The firing voltage in Fig. 5(a) was measured at a driving frequency of 20 kHz with a duty ratio of 30%. As shown in Fig. 5(a), with an increase in the address-electrode width, the firing voltages between

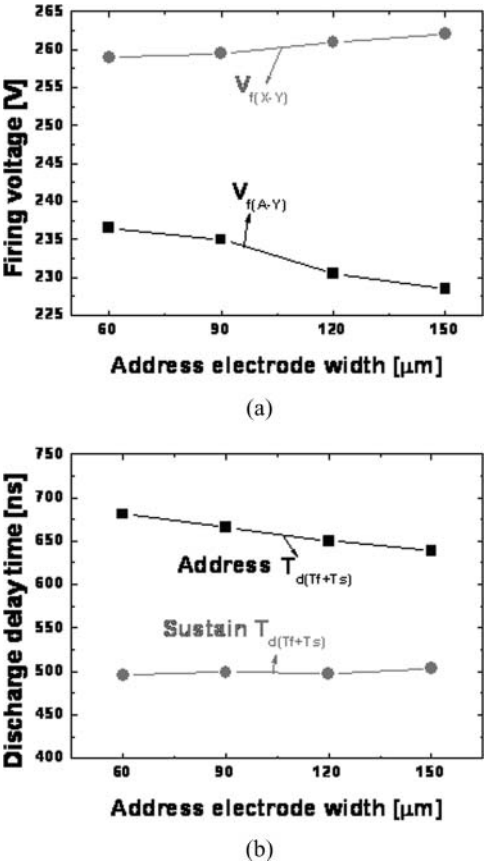

Figure 5. Comparison of (a) firing voltages between X-Y and A-Y electrodes and (b) address delay time during address and sustain discharge under various address electrode widths.

the A-Y electrodes decreased, whereas the firing voltages between the X-Y electrodes increased. The changes in the firing voltages, $V_{f(A\text{-}Y)}$ and $V_{f(X\text{-}Y)}$, showed the tendency contrary to the changes of the C_{AY} and C_{XY} caused by the variation in the address-electrode width. In particular, the increase in the address electrode width causes a decrease in the capacitance, C_{XY}, thereby resulting in the slight increase in the firing voltage between the X-Y electrodes.

Figure 5(b) also shows the changes in the address and sustain discharge delay times relative to the address-electrode width ranging from 60 to 150 μm where the address and sustain discharge delay times are the sum of formative delay time ($=T_f$) and statistical delay time ($=T_s$). The address and sustain discharge delay times were measured by detecting the infrared (IR) waveforms emitted under the same subfield using the photo sensor amplifier (Hamamatsu C6386). The address or sustain discharge delay time is defined as a time-period elapsed from the time when the scan pulse voltage falls to half of its maximum to the time when the emission signal reaches the ninety percent of its peak, which is measured by using an oscilloscope. As shown in Fig. 5(b), with an increase in the address-electrode width, the address discharge delay time decreased, whereas the sustain discharge delay time increased very slightly. In Fig. 5(b), the change in the sustain discharge delay was very small because the sustain pulse had a fast rising and falling slope and a higher voltage than that of the scan pulse. Whereas, the address discharge delay time was reduced by about 35 ns as a result of the capacitance variation, $\Delta C_{AY} = 0.0044$ pF.

Figure 6 shows the changes in the luminance under the full-white background relative to the address-electrode width ranging from 60 to 150 μm. As shown in Fig. 6, the luminance tended to increase with an increase in the address-electrode width, implying that the variation in the address electrode width affected the sustain discharge characteristics, especially luminance. This result confirmed that the grounded address electrode was able to affect the surface discharge produced between the two coplanar electrodes. The visible spectral intensity ranging from 370 to 730 nm was measured under various address electrode widths, and its result was shown in Fig. 7. As shown in Fig. 7, all spectral intensities of red, green and blue lights were increased as the address-electrode width became broaden.

The spectral intensities of IR rays (828 and 823 nm) and neon ray (585 nm) were measured relative to the address-electrode width ranging from 60 to 150 μm, and its result was shown in Figs. 8(a) and (b). In Figs. 8(a) and (b), the respective spectral intensity was normalized in such a manner that the value of the spectral intensity was 1 at the address

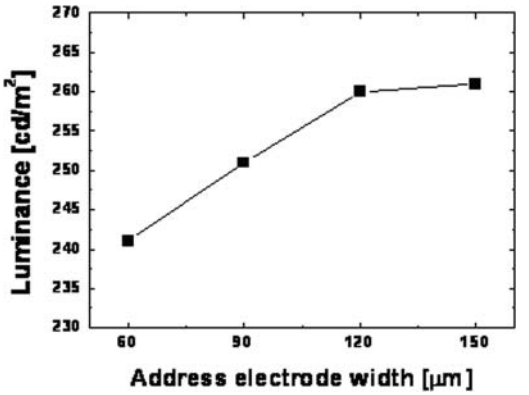

Figure 6. Comparison of luminance under full white background under various address electrode widths.

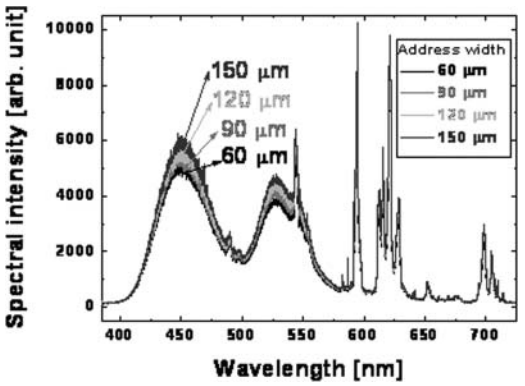

Figure 7. Comparison of spectral intensity of visible under various address electrode widths.

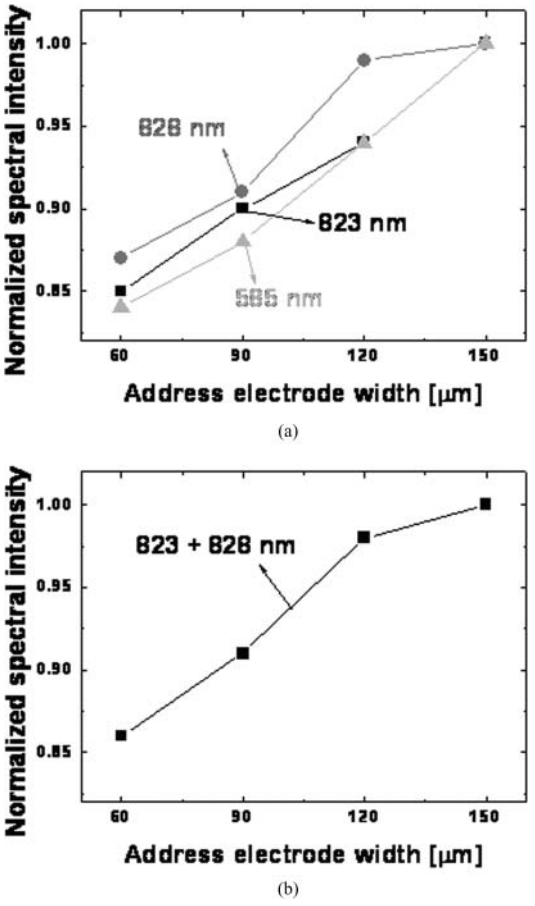

Figure 8. Comparison of (a) Xe (IR, 823 and 828 nm) and Ne (585 nm) spectral intensity and (b) Xe (IR, 823 adds to 828 nm) under various address electrode widths.

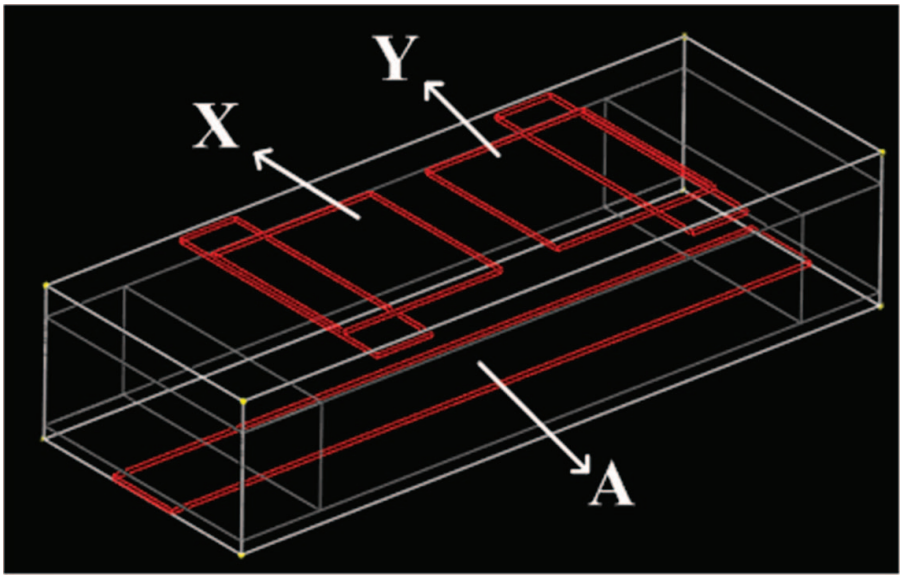

Figure 9. Schematic diagrams of cell structure for 3-D simulation.

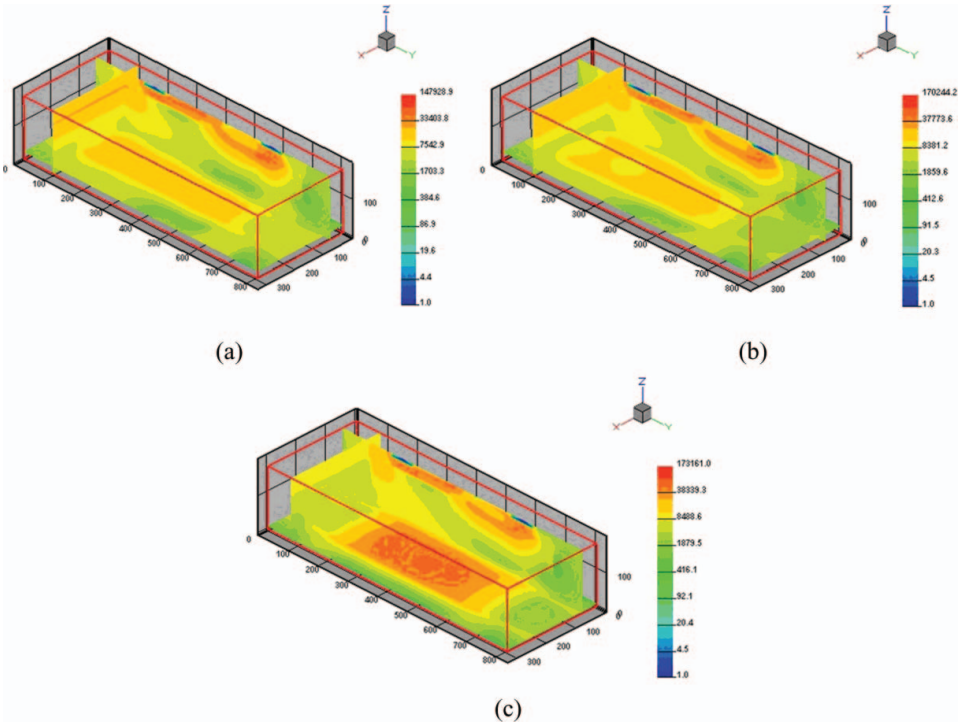

Figure 10. Comparison of electric field strength based on simulated results during sustain period under various address electrode widths. (a) 90 μm, (b) 130 μm, and (c) 150 μm.

electrode width of 150 μm. As shown in Fig. 8(a), the spectral intensities of not only IR rays but also neon ray increased with an increase in the address-electrode width. The increase in the address-electrode width caused an intensification of the electric field at a vicinity of address electrode, thereby resulting in an increase in the IR (828 and 823 nm) plus Ne emission. As shown in Figs. 6 and 8(b), the behaviors of the luminance and IR emission were very similar when increasing the address-electrode width. The variation in the luminance of Fig. 6 would result from the change in the sustain discharge characteristics such as the VUV emissions induced as a result of varying the address-electrode width.

3.2 Electric Field Strength and Xe Ion Distribution in Cell during Sustain Discharge Obtained from Simulation

To indentify the increase in the electric field at the vicinity of the address-electrode width of 150 μm during the discharge, the 3-D fluid model of plasma [3] was used in this simulation.

Figure 9 shows a schematic diagram of the cell structure for the 3-D simulation. Figure 10 shows the changes in the electric field strength distributed spatially within the cell as a result of varying the address-electrode width, whereas Fig. 11 shows the changes in the Xe ion distribution within the cell as a result of varying the address-electrode width.

As shown in Figs. 10 and 11, with an increase in the address-electrode width, the electric field strength and Xe ion distribution at the vicinity of address electrode were observed to be considerably increased. As the address-electrode width became broaden, the sustain discharge path was longer toward the address electrode, and the discharge volume was also enlarged, thereby resulting in an increase in the IR (828 and 823 nm) plus Ne emission. The

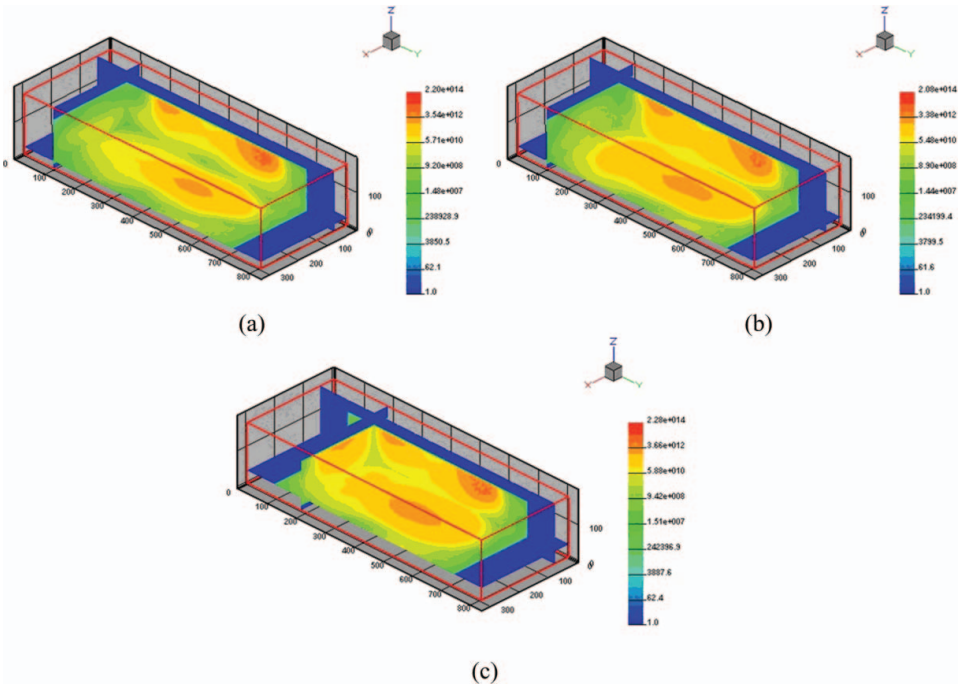

Figure 11. Comparison of Xe ion distribution based on simulated results during sustain period under various address electrode widths. (a) 90 μm, (b) 130 μm, and (c) 150 μm.

simulation result showed that as the address-electrode width increased, the electric field strength and Xe ion distribution at the vicinity of address electrode were intensified. As a consequence, the experimental results confirmed that the variation of the address-electrode width caused the changes in both the sustain and address discharge characteristics.

Conclusion

This paper investigates the variations in the capacitances among the electrodes and associated discharge characteristics in the 50 inch ac-PDP with a variable address-electrode width ranging from 60 to 150 μm at the intervals of 30 μm. As the address-electrode width was wider, the capacitance between the sustain and address electrodes ($=C_{AY}$) increased but the capacitance between the two sustain electrodes ($=C_{XY}$) decreased. The changes in the sustain and address discharge characteristics, such as a firing voltage, sustain voltage, discharge delay time, and luminance were also examined. The increase in the address-electrode width caused an increase in the firing voltage between the sustain electrodes, which was mainly due to the decrease in the capacitance between two sustain electrodes. Whereas, as the address-electrode width became broaden, the sustain discharge path was longer toward the address electrode, and the discharge volume was enlarged, thereby resulting in an increase in the IR (828 and 823 nm) plus Ne emission. The simulation results of monitoring the spatial distribution of electric field and Xe ion with respective to the address-electrode width have confirmed that the electric field strength and Xe ion distribution was intensified in the vicinity of address electrode, thereby resulting in an increase in the luminance and changing the address discharge characteristics. Finally, it is concluded that the area of grounded address electrode can have a significant influence on the sustain discharge stability by affecting the surface discharge produced between the two coplanar electrodes.

Acknowledgment

This work was supported in part by the Basic Science Research Program through the National Research Foundation of Korea (NRF) funded by the Korean Ministry of Education, Science and Technology (2012-0004506) and in part by Brain Korea 21 (BK21).

References

[1] Jeong, H. S., Murakami, Y., Seki, M., & Murakami, H. (2001). *IEEE Trans. Plasma Science*, *29*(3), 559–565.

[2] Jung, E. Y., Ahn, J. C., Kim, S. B., Suh, K. J., Heo, E. G., Lee, B. H., Lee, K. S., You, S. B., Jung, J. S., Park, J. Y., Song, S. B., & Lee, H. Y. (2005). *IDW'05*, *12*, 1551–1554.

[3] Song, S.-B., Park, P.-Y., Lee, H.-Y., Seo, J. H., & Kang, K. D. (2003). *Surface and Coating Technology*, *171*(1–3), 140–143.